Published in final edited form as:
J Immunol. 2006 April 1; 176(7): 4361–4368.

Lung-Restricted Macrophage Activation in the Pearl Mouse Model of Hermansky-Pudlak Syndrome[1]

Lisa R. Young[*,†], **Michael T. Borchers**[*,‡], **Holly L. Allen**[§], **Reta S. Gibbons**[§], and **Francis X. McCormack**[2,*]

[*]Department of Medicine, Division of Pulmonary and Critical Care, University of Cincinnati, Cincinnati, OH 45267

[†]Department of Pediatrics, Division of Pulmonary Medicine, Cincinnati Children's Hospital Medical Center, Cincinnati, OH 45229

[‡]Department of Environmental Health, Division of Environmental Genetics and Molecular Toxicology, University of Cincinnati, Cincinnati, OH 45267

[§]Department of Medicine, Division of Infectious Diseases, University of Cincinnati, Cincinnati, OH 45267

Abstract

Pulmonary inflammation, abnormalities in alveolar type II cell and macrophage morphology, and pulmonary fibrosis are features of Hermansky-Pudlak Syndrome (HPS). We used the naturally occurring "pearl" *HPS2* mouse model to investigate the mechanisms of lung inflammation observed in HPS. Although baseline bronchoalveolar lavage (BAL) cell counts and differentials were similar in pearl and strain-matched wild-type (WT) mice, elevated levels of proinflammatory (MIP1γ) and counterregulatory (IL-12p40, soluble TNFr1/2) factors, but not TNF-α, were detected in BAL from pearl mice. After intranasal LPS challenge, BAL levels of TNF-α, MIP1α, KC, and MCP-1 were 2- to 3-fold greater in pearl than WT mice. At baseline, cultured pearl alveolar macrophages (AMs) had markedly increased production of inflammatory cytokines. Furthermore, pearl AMs had exaggerated TNF-α responses to TLR4, TLR2, and TLR3 ligands, as well as increased IFN-γ/LPS-induced NO production. After 24 h in culture, pearl AM LPS responses reverted to WT levels, and pearl AMs were appropriately refractory to continuous LPS exposure. In contrast, cultured pearl peritoneal macrophages and peripheral blood monocytes did not produce TNF-α at baseline and had LPS responses which were no different from WT controls. Exposure of WT AMs to heat- and protease-labile components of pearl BAL, but not WT BAL, resulted in robust TNF-α secretion. Similar abnormalities were identified in AMs and BAL from another HPS model, pale ear *HPS1* mice. We conclude that the lungs of HPS mice exhibit hyperresponsiveness to LPS and constitutive and organ-specific macrophage activation.

Hermansky-Pudlak syndrome (HPS)[3] is a rare autosomal recessive disorder characterized by oculocutaneous albinism and a bleeding diathesis. Interstitial lung disease (ILD), which

[1]This work was supported by the following funding: National Institutes of Health (NIH) HL68861 (to F.X.M.), Procter Scholar Award, Cincinnati Children's Hospital Medical Center (to L.R.Y.), and NIH/National Institute of Environmental Health Sciences, Center for Environmental Genetics P30-ES06096-02 (to M.T.B.).

[2] Address correspondence and reprint requests to Dr. Francis X. McCormack, Division of Pulmonary and Critical Care, University of Cincinnati, 231 Albert Sabin Way, 6053 Medical Sciences Building, Cincinnati, OH 45267-0564. Frank.McCormack@uc.edu.

Disclosures
The authors have no financial conflict of interest.

exhibits histopathologic similarities to idiopathic pulmonary fibrosis (IPF), develops in most HPS patients who survive into adulthood (1, 2). Although IPF is increasingly recognized as a pauci-immune disorder with relatively mild degrees of leukocyte infiltration, other fibrotic lung diseases such as progressive hypersensitivity pneumonitis, sarcoidosis, desquamative interstitial pneumonitis, respiratory bronchiolitis-ILD, and connective tissue disease-related ILDs are often associated with robust cellular interstitial pneumonitis in the early stages of disease (3, 4).

Features which distinguish the histopathology of HPS from the usual interstitial pneumonia that is typical of IPF are lipid-filled, activated alveolar macrophages (AMs), lymphocyte infiltration, and hyperplastic, hypertrophic type II cells containing enlarged lamellar bodies (5, 6). Furthermore, recent evidence suggests that there are elevated levels of inflammatory cytokines and mononu-clear cells in the bronchoalveolar lavage (BAL) of HPS patients with mild lung function abnormalities (7). However, the link between these cellular and inflammatory abnormalities and pulmonary fibrosis remain poorly defined.

There are eight genetic loci known to be associated with HPS in humans and 14 HPS loci in mice (8, 9). Mutations in HPS genes result in defects in the biogenesis of lysosomes and lysosome-related intracellular organelles including melanosomes, platelet dense granules, and lamellar bodies (9–11). The *HPS2* protein product is the β3A subunit of the adaptor protein 3 (AP-3), a hetero-oligomeric complex which escorts proteins from the early trans-Golgi network to lysosome-related organelles (12–14). Mutations in AP-3 have been shown to result in instability and degradation of the AP-3 complex, leading to abnormalities in intra-cellular trafficking in a variety of cell types and organ systems (15–17). The “pale ear” *HPS1* mouse is the model for the most common HPS subtype, and although the precise function of the *HPS1* gene product (HPS1) remains unknown, it is also clearly critical for intracellular protein trafficking (9, 18, 19). Both pale ear and pearl mice have been shown to have structural abnormalities in alveolar cells that mimic those observed in humans with HPS, including foamy AMs and enlarged type II cells containing ceroid lipofuscin inclusions (13, 20, 21), but frank pulmonary fibrosis is not part of the mouse phenotype.

The macrophage alveolitis and elevated BAL levels of inflammatory cytokines in patients with HPS may contribute to pulmonary fibrosis. The hypothesis for this study was that aberrant macrophage activation or dampening plays a role in the dysregulated inflammation in HPS lungs. We used murine models to investigate AM function and the pulmonary inflammatory milieu in animals with mutations in HPS loci.

Materials and Methods

Mice

C57BL/6 mice were from Harlan and C3H/HeJ mice were from Charles River. Breeding pairs of pearl (*HPS2* mutation) and pale ear (*HPS1* mutation) mice were gifts from Dr. R. Swank (Roswell Park Cancer Institute, Buffalo, NY). C57BL/6 mice were used as the wild-type (WT) control (referred to as WT thereafter) for comparisons with HPS mice. Mice were housed in a barrier facility and studied using procedures approved by the University of Cincinnati Institutional Animal Care and Use Committee. Sentinel mice were tested periodically and were free of known viral and bacterial pathogens.

[3]Abbreviations used in this paper: HPS, Hermansky-Pudlak syndrome; ILD, inter-stitial lung disease; IPF, idiopathic pulmonary fibrosis; AM, alveolar macrophage; BAL, bronchoalveolar lavage; AP-3, adaptor protein 3; WT, wild type; i.n., intranasal; LDH, lactate dehydrogenase; LAL, *Limulus* amoebocyte lysate.

LPS-stimulated pulmonary inflammation

Mice were anesthetized to moderate depth with isofluorane (Forane; Ohmeda Caribe) by titration to unconsciousness and mild bradypnea. *Escherichia coli* J5 LPS (Sigma-Aldrich) was resuspended in PBS at a concentration of 10 mg/ml and repurified, where indicated, by phenol extraction (22). An LPS dose of 1 μg/animal (in 50 μl of PBS) was instilled intranasally (i.n.), and the animals were recovered in a clean cage.

Evaluation of airway and tissue cellular recruitment

At various time points after LPS instillation, mice were sacrificed by lethal pentobarbital injection followed by transection of the abdominal aorta. BAL was performed as described, after tracheostomy and intubation with a sterile 20-gauge adapter, and gentle instillation and aspiration of three 1-ml aliquots of 0.9% saline with 5 mM Tris. After separation of the BAL cells by low-speed centrifugation (450 × *g*, 10 min, 4°C), the BAL fluid was stored at –80°C until use. Cells were resuspended in PBS and counted using a Coulter counter or hemacytometer. A cell aliquot was spun onto glass slides using a cytocentrifuge (Shandon; speed = 300, 5 min), and slides were stained with DiffQuik (Sigma-Aldrich). The percentages of macrophages and neutrophils in BAL were determined by differential counting of a minimum of 200 cells.

BAL cytokine levels

Cytokine protein array—A dot-blot protein array technique was used for cytokine profiling (Raybiotech) according to the manufacturer's instructions. Briefly, membranes impregnated with multiple cytokines were blocked with the manufacturer's BSA buffer and incubated with undiluted BAL samples from pearl or WT mice for 2 h. After washing, a biotinylated anti-cytokine Ab mixture was added to the membrane and incubated for 2 h. Membranes were then washed, incubated with HRP-conjugated streptavidin, washed again, and then exposed to the manufacturer's peroxidase substrate. Chemiluminescent species were imaged by exposure of the membrane to film.

ELISA measurements of inflammatory cytokines—Cytokine protein concentrations in BAL and cell culture media were quantified by ELISA (murine Quantikine kits; R&D Systems), using the chromogenic substrate tetramethylbenzidine and analysis with a microtiter plate spectrophotometer at a wavelength of 450 nm. Lower limits of detection were as follows: 5.1 pg/ml TNF-α, 1.5 pg/ml MIP1α, 2.0 pg/ml MCP-1, 2.0 pg/ml KC, 2.5 pg/ml IL-12p70, 1.52 pg/ml MIP1γ, 5.0 pg/ml sTNFr1, 5.0 pg/ml sTNFr2, and 1.8 pg/ml IL-12p40. IL-12p40 was indistinguishable from IL-23p40 by the assay method used.

Isolation of mononuclear cells

Primary AMs were obtained from mice by BAL, and resident peritoneal macrophages were obtained by peritoneal lavage. To obtain peripheral blood monocytes for in vitro studies, mice were euthanized with CO_2, and murine blood was obtained by cardiac puncture. The mononuclear fraction was isolated on a Histopaque gradient, and monocytes were selected by adherence to plastic. Mononuclear cells from all sources were aliquoted in HBSS in sterile tissue culture plates and maintained in a humidified incubator at 37°C with 5% CO_2. Cells were allowed to adhere for 30 min before LPS (J5, 1 μg/ml; Sigma-Aldrich) was added. In other experiments, AMs were stimulated with the TLR2 ligand, Pam3Cys (1 μg/ml; EMC Micro-collections) or the TLR3 ligand, poly(I:C) (50 μg/ml; Amersham Biosciences). In some experiments, cells were cultured in DMEM with 10% FCS containing penicillin, streptomycin, and glutamine. At various time points, the cell culture media was collected, cleared of cellular debris by centrifugation, and stored at –80°C. Cell viability was assessed by trypan blue exclusion and lactate dehydrogenase (LDH) cytotoxicity assays

(CytoTox-ONE membrane integrity assay; Promega). Cytokine levels were then measured in the cell culture media supernatant by ELISA as described above.

Measurement of nitrite in cell culture supernatant

Primary alveolar or peritoneal macrophages (2.5×10^5 in the 96-well plates) were incubated for 24 h with and without the various additions as indicated. After plating, cells were challenged with IFN-γ (100 U/ml) for 3 h, followed by LPS (100 ng/ml) for 24 h. NO production was assessed by measuring the accumulation of nitrite in the culture media by the Griess reaction. Culture media (50 μl) was mixed with an equal volume of Griess reagent, composed of 1% sulfanilamide, 0.1% naphthalene diamine dihydrochloride, and 25% hydrochloric acid, according to the manufacturer's protocol (Promega). The plate was incubated for 10 min at room temperature and read in a plate spectrophotometer at 535 nm. Nitrite concentrations were determined from a standard curve using sodium nitrite at concentrations ranging from 1.5 to 100 μM.

Analysis of macrophage activating factors in BAL fluid

BAL fluid was obtained as described from control pearl and WT mice, cleared of cells by centrifugation, and then concentrated 10-fold through a 3000 Da Microcon (Amicon) filter. The protein content was measured by bicinchoninic acid assay (Pierce), and endotoxin levels were assessed by the *Limulus* amoebocyte lysate (LAL) assay (Cambrex). Primary AMs isolated from WT mice were stimulated in vitro with concentrated WT or pearl BAL fluid (final BAL protein concentration of 0.5 μg/μl) for 3 h. In some experiments, BAL fluid was boiled or treated with trypsin (1 μg, 37°C, 1 h) before addition to cells, as indicated. Cytokine levels in the cell culture media supernatant were measured by ELISA.

Statistics

Numeric data are presented as mean ± SD of the mean. Parametric data were evaluated using the Student *t* test, or by one-way ANOVA for comparison of more than two groups.

Results

Pearl mice have evidence of basal inflammatory dysregulation

Pulmonary inflammation is present in the lungs of patients with early HPS lung disease (7). To determine whether HPS mouse models exhibited similar inflammatory abnormalities, BAL fluid was evaluated from 6- to 8-wk-old pearl, pale ear, and strain-matched WT mice (Fig. 1). HPS mice had significantly increased baseline BAL levels of IL-12p40, MIP1γ, and the soluble TNFRs sTNFr1 and sTNFr2 (data not shown), whereas TNF-α, MIP1α, IL-1β, IL-12p70, IFN-γ, and IL-10 were all undetectable in BAL from unchallenged HPS or WT mice.

Pearl mice have elevated inflammatory markers in BAL after i.n. LPS challenge

To determine whether HPS mice have an aberrant acute pulmonary response to inflammatory stimuli, mice were challenged with a single i.n. endotoxin exposure. A cytokine array technique was used to screen for differences in cytokine levels in BAL fluid and lung tissue homogenate from LPS-challenged pearl and strain-matched WT mice. As shown in a representative array (Fig. 2*A*), 3 h after i.n. LPS exposure, signals corresponding to MCP-1, KC, RANTES, and several other cytokines were visibly increased on the membranes exposed to BAL fluid from pearl mice relative to those from age- and strain-matched WT controls. Specific ELISAs were then used to quantify several of the cytokine protein elevations suggested by the array screens. BAL TNF-α levels (Fig. 2*B*) were similar in pearl and WT mice at baseline and at 1 h after LPS challenge, but remained elevated in

pearl mice from 3 h postchallenge through 24 h. Similarly, MIP1α levels were undetectable in baseline BAL fluid, 2-fold greater in pearl mice than WT controls 3 h after i.n. LPS challenge (Fig. 2*C*), 6-fold greater after 8 h (not shown), and 2-fold greater at the 24 h time point ($p < 0.001$; not shown). BAL levels of MCP-1 also remained elevated in pearl mice for up to 24 h after i.n. LPS challenge (data not shown). At 3 h post-LPS challenge, KC levels were 2.5-fold greater in pearl than WT mice (868 ± 180 vs 353 ± 88 pg/ml, respectively; $p < 0.001$).

To determine whether the observed cytokine differences were also associated with other HPS mutations, we examined the inflammatory responses of the pale ear (ep) *HPS1* mouse, a model for the most common human HPS subtype (18, 23). Three hours after i.n. LPS challenge, pale ear mice also had significantly greater levels of MIP1α (Fig. 2*C*) and TNF-α (7032 ± 578 pg/ml for pale ear vs 4253 ± 320 pg/ml for WT; $p = 0.002$) in BAL than WT mice.

Pearl mice have an abnormal pulmonary cellular inflammatory response to i.n. endotoxin administration

Patients with HPS have been found to have increased numbers of BAL macrophages (including “foamy” macrophages), and lung histology from HPS patients shows a macrophage and lymphocyte predominant interstitial infiltrate (5). To evaluate the mechanisms of increased cellularity in HPS and determine whether HPS mouse models shared this phenotype, we examined lung and airway leukocyte populations in pearl and WT mice. In unchallenged, 6- to 8-wk-old animals, pearl AMs were enlarged and “foamy” in appearance (Fig. 3*A*), but there were no significant differences in total BAL cell numbers (Fig. 3*B*) or composition between pearl and WT mice (Fig. 3*C*). Therefore, in the pearl mouse, abnormalities in inflammatory cytokine production (Figs. 1 and 2) are not accompanied by abnormalities in alveolar cell composition at baseline.

After LPS challenge, significant unanticipated differences were observed in the inflammatory cells recruited to both the airways and lung parenchyma of pearl mice. Pearl mice had a 2-fold excess number and proportion of BAL macrophages, while pale ear mice had a significant, though less prominent increase in BAL macrophages in comparison to WT controls (Fig. 3*C*). However, pearl mice had only half as many neutrophils in the airspace 3 h after exposure to i.n. LPS compared with WT controls (Fig. 3, *A* and *C*). Numbers of BAL neutrophils in pearl and WT mice were similar 8 h after LPS exposure (data not shown). Furthermore, the neutrophil-trafficking delay was specific to AP3-deficient pearl mice, as LPS-induced neutrophil recruitment in pale ear mice was similar to WT mice (Fig. 3*C*).

Isolated murine HPS AMs, but not peritoneal macrophages or peripheral blood monocytes, have dysregulated inflammatory cytokine production and LPS responsiveness

We isolated AMs from pearl, pale ear, and WT mice and studied LPS responsiveness ex vivo. Inflammatory cytokines such as TNF-α (Fig. 4*A*) and MIP1α, MCP-1, and KC (data not shown) were produced at detectable levels by pearl and pale ear, but not by WT, AMs in culture at baseline. After challenge with LPS, pearl and pale ear AMs had significantly greater LPS responsiveness than WT AMs (4-fold greater for TNF-α, 6-fold greater for MIP1α; $p < 0.001$ for both). Levels of IL-12p40 and the soluble TNFRs, sTNFr1 and sTNFr2 (not shown), were markedly elevated in the media of unstimulated pearl AMs after 24 h in culture compared with WT AMs (Fig. 4, *B* and *C*). These factors were not detectable in media from either pearl or WT AMs after only 3 h in culture, however.

To determine whether the aberrant cytokine responsiveness of pearl monocytes was organ specific, resident peritoneal macrophages and peripheral blood monocytes from pearl and

WT mice were isolated and evaluated ex vivo. In contrast to pearl AMs, no significant TNF-α was detected in media from either pearl or WT peritoneal macrophages or monocytes after 3 h in culture at baseline. Furthermore, after LPS challenge, TNF-α production was no different for peritoneal macrophages and peripheral blood monocytes from pearl mice than from WT mice (Fig. 4*A*). These data demonstrate that the abnormal cytokine responses of pearl mononuclear cells are specific to AMs.

Murine HPS AMs exhibit enhanced NO production in response to LPS challenge

To determine whether the abnormal pearl AM activation was specific to cytokine production or reflective of more general AM activation, NO production by pearl and WT AMs was determined ex vivo by measuring accumulated nitrite in the media from cultured macrophages. At baseline, NO was barely detectable in the media from unstimulated pearl or WT AMs that had been cultured for 24 h. Furthermore, LPS stimulation alone induced inconsistent and low level NO production from WT AMs under these conditions at 24 h, as has been reported (data not shown) (24). Therefore, macrophages were costimulated with IFN-γ/LPS, which resulted in 4-fold more nitrite accumulation from pearl AMs than WT AMs. In contrast, IFN-γ/LPS-induced nitrite production from pearl peritoneal macrophages was not different from WT peritoneal macrophages (Fig. 5).

Pearl AM hyperresponsiveness is not limited to TLR4-mediated mechanisms

We investigated whether pearl AM hyperresponsiveness was specific to LPS challenge. Pearl AMs were isolated and challenged in vitro with Pam3Cys, a bacterial lipoprotein that binds to TLR2, and poly(I:C), a synthetic polynucleotide ligand for TLR3. Pearl AMs produced 3-fold greater levels of TNF-α in response to Pam3Cys than did WT AMs (2040 ± 88 vs 671 ± 137 pg/ml; $p < 0.01$) (Fig. 6). When challenged with poly(I:C), TNF-α production was 4-fold greater from pearl than WT AMs (1840 ± 320 vs 437 ± 100 pg/ml; $p < 0.01$).

Pearl AM hyperresponsiveness is lost after 24 h in culture

To determine whether elevated cytokine levels were related to an intrinsic failure of pearl AMs to down-regulate inflammatory responses, we examined TNF-α production by AMs challenged with LPS at various time points in culture. Pearl, but not WT, AMs produced elevated levels of TNF-α for the first 24 h in culture, much less in the second 24 h, and only baseline levels from 48 to 72 h (Fig. 7*A*, ■ and □). Furthermore, during the first 24 h ex vivo, pearl AMs were hyperresponsive to LPS challenge as compared with WT AMs (4534 ± 191vs 2300 ± 236 pg/ml; $p < 0.005$) (Fig. 7*A*, ● and ○). When the LPS challenge was withdrawn, TNF-α production declined precipitously in both pearl and WT AMs. Moreover, both pearl and WT AMs became refractory to persistent LPS exposure in vitro, with progressively diminishing TNF-α levels from 24 to 72 h despite continuous incubation with LPS (Fig. 7*A*, ▲ and △).

The hyperresponsiveness of pearl AMs was extinguished by 48 h in culture. WT AMs had consistent peak levels of TNF-α production whether challenge occurred at baseline (Fig. 7*A*), 24 h (Fig. 7*B*), or at 48 h in culture (Fig. 7*B*). In contrast, pearl AMs exhibited excess TNF-α production in response to LPS challenge at time 0 (Fig. 7*A*), but the LPS-induced TNF-α response of pearl AMs reverted to WT levels when the LPS challenge was initiated at 24 or 48 h in culture (Fig. 7*B*). Cell viability and integrity was similarly maintained in pearl and WT AMs as assessed by trypan blue exclusion and lack of LDH release.

Protein components of BAL from pearl mice activate WT macrophages

Based on the findings that pearl AMs exhibited exaggerated responses to LPS challenge, that hyperresponsiveness dissipated after 24 h in cell culture, and that peritoneal macrophages and peripheral monocytes had normal inflammatory responses, we reasoned that factor(s) in the pearl lung environment may be responsible for pearl AM activation. To test this hypothesis, BAL was obtained from control pearl and WT mice, concentrated, and verified to be endotoxin-free by LAL assay. TNF-α, MIP1α, and IFN-γ were not detected in the concentrated pearl BAL by ELISA. When primary AMs from WT mice were stimulated in vitro with concentrated BAL fluid (total protein concentration 0.5 μg/μl) for 3 h, WT AMs produced high levels of TNF-α (330 ± 95 pg/ml) in response to exposure to pearl, but not WT, BAL(13 ± 41 pg/ml) (Fig. 8). Additionally, AMs from C3H/HeJ mice, which contain a TLR4 mutation and thus do not respond to LPS, were also activated by exposure to pearl BAL (Fig. 8). This finding in HeJ AMs confirms that LPS contamination was not responsible for the macrophage activation, and that the mechanism of activation is TLR4 independent. Boiling or protease treatment of pearl BAL fluid blocked the macrophage-activating activity. As a control, we verified that residual trypsin activity was not degrading the TNF-α produced by AMs by incubating trypsin alone at 37°C for 1 h and then adding it to cultured pearl AMs before measurement of TNF-α levels (data not shown). Concentrated BAL fluid from pale ear mice also induced marked TNF-α production from WT AMs (Fig. 8). In the presence of neutralizing Ab to TNF-α, pearl, but not WT BAL, induced high levels of MIP1α production from WT AMs (data not shown). Preincubation of pearl BAL with specific neutralizing Abs to KC, IFN-γ, IL-12p40, or CXCR2 also did not dampen pearl BAL-induced cytokine release from AMs (data not shown).

Discussion

These experiments demonstrate that HPS mouse models have a pulmonary phenotype that is characterized by baseline elevations in inflammatory cytokines and counterregulatory factors, abnormal cellular recruitment, and exaggerated cytokine responses to endotoxin challenge. Abnormal cytokine responses were also found in isolated alveolar, but not peritoneal, macrophages and decayed with time in culture, suggesting that factors unique to the lung environment promote the activated state.

HPS is the most penetrant genetic disorder of pulmonary fibrosis in adults, as virtually all patients who survive to adulthood develop fibrotic lung disease (2, 25). HPS1 is most common human geno-type, and accounts for the majority of ILD reported in HPS. Clinically apparent lung disease has been reported to occur in the fourth or fifth decades of life (1, 2, 25), and the role of environmental influences on disease progression is not known. Although the four reported patients with HPS2 are younger in age than HPS1 and HPS4 patients with pulmonary fibrosis, mild pulmonary fibrosis was described in two cases (26, 27).

The cellular effectors of fibrosis in HPS are uncertain. Although HPS AMs are enlarged, structurally abnormal, and contain ceroid lipofuscin, the data presented is the first demonstration that these cellular derangements are associated with aberrant macrophage function. The presence of AM hyperresponsiveness in both pearl and pale ear mice demonstrates that these inflammatory abnormalities are not genotype-specific, at least in mouse models. Genetic abnormalities of a number of key elements required for protein trafficking from the ER to lysosome-related organelles can cause HPS (9, 11), and determination of how trafficking defects potentially lead to AM dysfunction and fibrosis is a fruitful area for further study.

Despite the presence of equivalent numbers of AMs, we have found that 6- to 8-wk-old pearl mice have baseline elevations of MIP1γ as compared with WT mice. The HPS mice

also have acute elevations in many proinflammatory cytokines in response to endotoxin challenge, including TNF-α and MIP1α, which function to initiate the inflammatory cascade and cytokine-mediated cellular recruitment. MIP1α is a primary monocyte chemoattractant, but has also been shown to have effects on other leukocyte populations (28), while MCP-1, which is produced by both macrophages and epithelial cells, is strongly chemotactic for macrophages and also enhances Th2 lymphocyte development (29–31). The proinflammatory state of AMs and/or other alveolar cells promotes the deployment of counterregulatory, anti-inflammatory factors such as IL-12p40 and the soluble TNF receptors, which are present in elevated levels even at baseline in pearl BAL and from isolated pearl AMs. It is unknown whether these mechanisms also contribute to the excess macrophage accumulation in LPS-challenged HPS mice, or to the macrophage and lymphocyte accumulation that has been reported in the lungs of HPS patients (5).

We found that both pearl and pale ear AMs exhibit constitutive inflammatory cytokine production in vitro. These data suggest that murine HPS AMs have an aberrant activation state at baseline, leading to both an exaggerated inflammatory response and to production of anti-inflammatory mediators, and suggests that AMs are a cellular source of these mediators in vivo. Furthermore, we have found that murine HPS AMs have exaggerated LPS-responsiveness, as assessed by both cytokine production and release of NO.

The implications of the exaggerated pulmonary LPS response in HPS mice are uncertain, and we have not yet investigated the consequences of repetitive environmental stimuli, which may more closely mimic the environmental pulmonary challenges that patients with HPS experience. The innate immune response to inhaled LPS and microorganisms must be tightly regulated to avoid damaging host tissues. The AM plays a central role in lung host defense through both effector and regulatory functions. Upon exposure to pathogens, AMs express cytokines that influence recruitment and activation of inflammatory cells and modify adaptive immune responses in a pathogen-selective fashion. LPS from Gram-negative organisms initiates the pulmonary inflammatory response through TLR signaling. In serum and perhaps in the lung, LPS first binds to soluble LPS-binding protein, followed by transfer to a cell surface receptor complex consisting of CD-14, MD-2, and the TLR4 (32). Autophosphorylation of the cytoplasmic domain of TLR4 results in signaling through MyD88, as well as via a MyD88-independent pathway, which converge on NF-κB. Nuclear translocation of NF-κB results in increased production of TNF-α mRNA and protein, as well as other cytokines (33).

There are several levels of regulation of TLR pathways, including soluble decoy receptors, down-regulation of cell surface receptors, intracellular inhibitors of LPS signaling such as suppressor of cytokine signaling and IL-1R-associated kinase-M, negative regulation of TLR gene transcription, degradation of TLR proteins, or activation induced apoptosis (34). Our finding of excessive TNF-α production from HPS murine AMs might suggest an abnormality in the negative regulation of pathways required for response to inflammatory stimuli. However, given that pearl AMs are also hyperresponsive to TLR2 and TLR3 stimuli, the mechanism must also involve TLR4-independent and Myd88-independent signaling pathways. This aberrant response appears to be due to an abnormality in basal activation in vivo, rather than to a failure to down-regulate inflammatory responses, as pearl AMs have normal dampening mechanisms upon LPS withdrawal and are appropriately refractory to continuous LPS challenge in vitro. The observed excess deployment of anti-inflammatory factors such as the soluble TNFRs and IL-12p40 may constitute a counterregulatory mechanism for murine HPS AMs which are constitutively activated through intrinsic or extrinsic mechanisms.

Persistent inflammation has been shown to contribute to the pathogenesis of fibrosis in multiple organs, including the gut, liver, and kidney (35–41). The imbalance of proinflammatory and counterregulatory factors, including TNF-α and soluble TNFRs have also been implicated in the pathogenesis of a variety of fibrotic disorders in both humans and in animal models (35–37). Specifically, overexpression of IL-12p40-related cytokines have been reported in fibrogenic Th1-mediated autoimmune and chronic inflammatory diseases, including glomerulonephritis (39), as well as in experimental models of pulmonary fibrosis (42). Therefore, our findings of excessive production of TNF-α, sTNFr1, sTNFr2, and IL-12p40 in pearl and pale ear mice and from their AMs ex vivo suggest a potential link between the pro and anti-inflammatory imbalance and fibrogenesis. Certainly further studies are required to determine whether macrophage activation plays a causative role in fibrotic lung disease in HPS.

Pearl and pale ear HPS mouse models do not exhibit spontaneous fibrosis at the age at which our experiments were performed, and, in fact, unchallenged HPS mice develop airspace enlargement over time (21). Although others have reported that aged pearl mice develop expansion of interstitial septa by excess collagen fibrils (43), that pale ear mice have an increased fibrotic responses to silica challenge (44), and that the lungs of double-mutant HPS1/HPS2 (*ep/pe*) mice contain a significant increase in hydroxyproline content compared with controls (21), whether the phenotype of HPS mouse models includes susceptibility to pulmonary fibrosis remains controversial.

In contrast to the similarities in AM recruitment in pearl and pale ear mice, we have demonstrated that the neutrophil trafficking defects are clearly specific to the *HPS2* genotype in mice, as pale ear *HPS1* mice have normal neutrophil trafficking. It remains unknown whether pearl neutrophils have intrinsic abnormalities of key proteins required for cellular migration, such as in Rac, selec-tins, or integrins, affecting cell-to-cell signaling, movement, or adhesion, respectively. It is also possible that pearl epithelium or macrophages fail to release critical factors required for neutrophil recruitment in response to LPS challenge. The demonstration of mistrafficking of neutrophil elastase to the plasma membrane in AP-3-deficient dogs with “Gray Collie syndrome” (canine cyclical neutropenia) suggests a potential role for mistargeted matrix pro-teases in neutrophil-trafficking abnormalities in pearl mice (45, 46). Studies are underway in the laboratory to investigate the mechanisms of the neutrophil-trafficking abnormality in pearl mice.

Two lines of evidence demonstrate that pearl monocyte hyperresponsiveness is restricted to the lung environment. First, pearl AMs, but not peritoneal macrophages or peripheral monocytes, are constitutively activated and have exaggerated inflammatory responses to endotoxin challenge. AM-specific activation was also apparent with respect to nitrite production. The mechanism of pearl AM hyperresponsiveness is unknown, but may reflect up-regulation of cell surface receptors, or perhaps loss of intracellular or extracellular repressors. Second, pearl AMs lose their hyperresponsiveness after only 1 day in culture. One potential explanation for this observation is that removal from exposure to a factor or factors that are unique to the lung compartment extinguishes the heightened inflammatory tone of pearl AMs. However, primary AMs de-differentiate and down-regulate cell surface receptors in vitro (47), and we cannot exclude cell culture artifacts as the basis for loss of pearl AM hyperresponsiveness.

Potential mechanisms for lung-restricted AM activation were examined. We found that a heat- and protease-sensitive BAL factor (or factors) from both pearl and pale ear BAL induces TNF-α and MIP1α production from WT AMs. This effect is not due to LPS contamination and is not mediated through the TLR4 pathway, because AMs from HeJ mice are activated by pearl BAL. These data suggest that protein components of pearl BAL play a

role in AM hyperresponsiveness, but additional experiments are needed to determine whether the factor is a chemokine, cytokine, or a novel factor. Production of the factor is not genotype specific because it is generated by both pearl and pale ear mice. The most likely cellular sources of this activating factor are the alveolar epithelium, the AM, or both. As such, this finding of macrophage-activating activity in pearl and pale ear BAL does not preclude the possibility of intrinsic functional abnormalities in HPS macrophages. Furthermore, although pearl AMs produce abundant TNF-α ex vivo, TNF-α is not detectable in concentrated BAL from pearl mice at baseline. It is possible that the isolation and cell culture process may enhance pearl but not WT macrophage activation.

In summary, we conclude that the lungs of HPS mice exhibit hyperresponsiveness to LPS, altered inflammatory cell trafficking, and constitutive AM activation. Further investigation of the dys-regulated inflammatory state and AM activation in HPS mice may provide insights into the early inflammation and midlife fibrosis seen in the lungs of HPS patients.

Acknowledgments

We thank Dr. Richard Swank for providing the pearl and pale ear mice.

References

1. Gahl WA, Brantly M, Kaiser-Kupfer MI, Iwata F, Hazelwood S, Shotelersuk V, Duffy LF, Kuehl EM, Troendle J, Bernardini I. Genetic defects and clinical characteristics of patients with a form of oculocutaneous albinism (Hermansky-Pudlak syndrome). N. Engl. J. Med. 1998; 338:1258–1264. [PubMed: 9562579]
2. Brantly M, Avila NA, Shotelersuk V, Lucero C, Huizing M, Gahl WA. Pulmonary function and high-resolution CT findings in patients with an inherited form of pulmonary fibrosis, Hermansky-Pudlak syndrome, due to mutations in HPS-1. Chest. 2000; 117:129–136. [PubMed: 10631210]
3. Rossi GA, Bitterman PB, Rennard SI, Ferrans VJ, Crystal RG. Evidence for chronic inflammation as a component of the interstitial lung disease associated with progressive systemic sclerosis. Am. Rev. Respir. Dis. 1985; 131:612–617. [PubMed: 3994157]
4. Fischer B, Morgenroth K. Ultrastructural study on human lung in alveolitis versus pulmonary fibrosis. Clin. Invest. 1993; 71:452–460.
5. Nakatani Y, Nakamura N, Sano J, Inayama Y, Kawano N, Yamanaka S, Miyagi Y, Nagashima Y, Ohbayashi C, Mizushima M, et al. Interstitial pneumonia in Hermansky-Pudlak syndrome: significance of florid foamy swelling/degeneration (giant lamellar body degeneration) of type-2 pneumocytes. Virchows Arch. 2000; 437:304–313. [PubMed: 11037352]
6. White DA, Smith GJ, Cooper JA Jr. Glickstein M, Rankin JA. Hermansky-Pudlak syndrome and interstitial lung disease: report of a case with lavage findings. Am. Rev. Respir. Dis. 1984; 130:138–141. [PubMed: 6742598]
7. Rouhani F, Gahl WA, Tobias C, Jolley C, Brantly M. Cellular and cytokine characteristics of epithelial lining fluid in individuals with pulmonary fibrosis who harbor A 16-BP duplication in the Hermansky-Pudlak syndrome gene. Am. J. Respir. Crit. Care Med. 2000; 164:A503.
8. Morgan NV, Pasha S, Johnson CA, Ainsworth JR, Eady RA, Dawood B, McKeown C, Trembath RC, Wilde J, Watson SP, Maher ER. A germline mutation in BLOC1S3/reduced pigmentation causes a novel variant of Hermansky-Pudlak syndrome (HPS8). Am. J. Hum. Genet. 2006; 78:160–166. [PubMed: 16385460]
9. Li W, Rusiniak ME, Chintala S, Gautam R, Novak EK, Swank RT. Murine Hermansky-Pudlak syndrome genes: regulators of lysosome-related organelles. Bioessays. 2004; 26:616–628. [PubMed: 15170859]
10. Swank RT, Novak EK, McGarry MP, Rusiniak ME, Feng L. Mouse models of Hermansky Pudlak syndrome: a review. Pigm. Cell Res. 1998; 11:60–80.
11. Dell'Angelica EC. The building BLOC(k)s of lysosomes and related organelles. Curr. Opin. Cell Biol. 2004; 16:458–464. [PubMed: 15261680]

12. Dell'Angelica EC, Shotelersuk V, Aguilar RC, Gahl WA, Bonifacino JS. Altered trafficking of lysosomal proteins in Hermansky-Pudlak syndrome due to mutations in the β3A subunit of the AP-3 adaptor. Mol. Cell. 1999; 3:11–21. [PubMed: 10024875]
13. Feng L, Seymour AB, Jiang S, To A, Peden AA, Novak EK, Zhen L, Rusiniak ME, Eicher EM, Robinson MS, et al. The β3A subunit gene (Ap3b1) of the AP-3 adaptor complex is altered in the mouse hypopigmentation mutant pearl, a model for Hermansky-Pudlak syndrome and night blindness. Hum. Mol. Genet. 1999; 8:323–330. [PubMed: 9931340]
14. Feng L, Rigatti BW, Novak EK, Gorin MB, Swank RT. Genomic structure of the mouse Ap3b1 gene in normal and pearl mice. Genomics. 2000; 69:370–379. [PubMed: 11056055]
15. Clark RH, Stinchcombe JC, Day A, Blott E, Booth S, Bossi G, Hamblin T, Davies EG, Griffiths GM. Adaptor protein 3-dependent microtubule-mediated movement of lytic granules to the immunological synapse. Nat. Immunol. 2003; 4:1111–1120. [PubMed: 14566336]
16. Sugita M, Cao X, Watts GF, Rogers RA, Bonifacino JS, Brenner MB. Failure of trafficking and antigen presentation by CD1 in AP-3-deficient cells. Immunity. 2002; 16:697–706. [PubMed: 12049721]
17. Huizing M, Sarangarajan R, Strovel E, Zhao Y, Gahl WA, Boissy RE. AP-3 mediates tyrosinase but not TRP-1 trafficking in human melanocytes. Mol. Biol. Cell. 2001; 12:2075–2085. [PubMed: 11452004]
18. Gardner JM, Wildenberg SC, Keiper NM, Novak EK, Rusiniak ME, Swank RT, Puri N, Finger JN, Hagiwara N, Lehman AL, et al. The mouse pale ear (ep) mutation is the homologue of human Hermansky-Pudlak syndrome. Proc. Natl. Acad. Sci. USA. 1997; 94:9238–9243. [PubMed: 9256466]
19. Tang X, Yamanaka S, Miyagi Y, Nagashima Y, Nakatani Y. Lung pathology of pale ear mouse (model of Hermansky-Pudlak syndrome 1) and beige mouse (model of Chediak-Higashi syndrome): severity of giant lamellar body degeneration of type II pneumocytes correlates with interstitial inflammation. Pathol. Int. 2005; 55:137–143. [PubMed: 15743322]
20. Zhen L, Jiang S, Feng L, Bright NA, Peden AA, Seymour AB, Novak EK, Elliott R, Gorin MB, Robinson MS, Swank RT. Abnormal expression and subcellular distribution of subunit proteins of the AP-3 adaptor complex lead to platelet storage pool deficiency in the pearl mouse. Blood. 1999; 94:146–155. [PubMed: 10381507]
21. Lyerla TA, Rusiniak ME, Borchers M, Jahreis G, Tan J, Ohtake P, Novak EK, Swank RT. Aberrant lung structure, composition, and function in a murine model of Hermansky-Pudlak syndrome. Am. J. Physiol. 2003; 285:L643–L653.
22. Hirschfeld M, Ma Y, Weis JH, Vogel SN, Weis JJ. Cutting edge: repurification of lipopolysaccharide eliminates signaling through both human and murine Toll-like receptor 2. J. Immunol. 2000; 165:618–622. [PubMed: 10878331]
23. Feng GH, Bailin T, Oh J, Spritz RA. Mouse pale ear (ep) is homologous to human Hermansky-Pudlak syndrome and contains a rare “AT-AC” intron. Hum. Mol. Genet. 1997; 6:793–797. [PubMed: 9158155]
24. Stamme C, Walsh E, Wright JR. Surfactant protein A differentially regulates IFN-γ- and LPS-induced nitrite production by rat alveolar macrophages. Am. J. Respir. Cell Mol. Biol. 2000; 23:772–779. [PubMed: 11104730]
25. Avila NA, Brantly M, Premkumar A, Huizing M, Dwyer A, Gahl WA. Hermansky-Pudlak syndrome: radiography and CT of the chest compared with pulmonary function tests and genetic studies. Am. J. Roentgenol. 2002; 179:887–892. [PubMed: 12239031]
26. Huizing M, Scher CD, Strovel E, Fitzpatrick DL, Hartnell LM, Anikster Y, Gahl WA. Nonsense mutations in ADTB3A cause complete deficiency of the β3A subunit of adaptor complex-3 and severe Hermansky-Pudlak syndrome type 2. Pediatr. Res. 2002; 51:150–158. [PubMed: 11809908]
27. Shotelersuk V, Dell'Angelica EC, Hartnell L, Bonifacino JS, Gahl WA. A new variant of Hermansky-Pudlak syndrome due to mutations in a gene responsible for vesicle formation. Am. J. Med. 2000; 108:423–427. [PubMed: 10759101]
28. Ritter LM, Bryans M, Abdo O, Sharma V, Wilkie NM. MIP1 α nuclear protein (MNP), a novel transcription factor expressed in hematopoietic cells that is crucial for transcription of the human MIP-1 α gene. Mol. Cell. Biol. 1995; 15:3110–3118. [PubMed: 7760807]

29. Boring L, Gosling J, Chensue SW, Kunkel SL, Farese RV Jr. Broxmeyer HE, Charo IF. Impaired monocyte migration and reduced type 1 (Th1) cytokine responses in C-C chemokine receptor 2 knockout mice. J. Clin. Invest. 1997; 100:2552–2561. [PubMed: 9366570]

30. Chensue SW, Warmington KS, Ruth JH, Sanghi PS, Lincoln P, Kunkel SL. Role of monocyte chemoattractant protein-1 (MCP-1) in Th1 (mycobacterial) and Th2 (schistosomal) antigen-induced granuloma formation: relationship to local inflammation, Th cell expression, and IL-12 production. J. Immunol. 1996; 157:4602–4608. [PubMed: 8906839]

31. Matsukawa A, Lukacs NW, Standiford TJ, Chensue SW, Kunkel SL. Adenoviral-mediated overexpression of monocyte chemoattractant protein-1 differentially alters the development of Th1 and Th2 type responses in vivo. J. Immunol. 2000; 164:1699–1704. [PubMed: 10657613]

32. Poltorak A, He X, Smirnova I, Liu MY, Van Huffel C, Du X, Birdwell D, Alejos E, Silva M, Galanos C, et al. Defective LPS signaling in C3H/HeJ and C57BL/10ScCr mice: mutations in TLR4 gene. Science. 1998; 282:2085–2088. [PubMed: 9851930]

33. Medzhitov R, Preston-Hurlburt P, Kopp E, Stadlen A, Chen C, Ghosh S, Janeway CA Jr. MyD88 is an adaptor protein in the hToll/IL-1 receptor family signaling pathways. Mol. Cell. 1998; 2:253–258. [PubMed: 9734363]

34. Nakagawa R, Naka T, Tsutsui H, Fujimoto M, Kimura A, Abe T, Seki E, Sato S, Takeuchi O, Takeda K, et al. SOCS-1 participates in negative regulation of LPS responses. Immunity. 2002; 17:677–687. [PubMed: 12433373]

35. Marini M, Bamias G, Rivera-Nieves J, Moskaluk CA, Hoang SB, Ross WG, Pizarro TT, Cominelli F. TNF-α neutralization ameliorates the severity of murine Crohn's-like ileitis by abrogation of intestinal epithelial cell apoptosis. Proc. Natl. Acad. Sci. USA. 2003; 100:8366–8371. [PubMed: 12832622]

36. Noguchi M, Hiwatashi N, Liu Z, Toyota T. Secretion imbalance between tumour necrosis factor and its inhibitor in inflammatory bowel disease. Gut. 1998; 43:203–209. [PubMed: 10189845]

37. Khan SB, Cook HT, Bhangal G, Smith J, Tam FW, Pusey CD. Antibody blockade of TNF-α reduces inflammation and scarring in experimental crescentic glomerulonephritis. Kidney Int. 2005; 67:1812–1820. [PubMed: 15840028]

38. Kitching AR, Tipping PG, Kurimoto M, Holdsworth SR. IL-18 has IL-12-independent effects in delayed-type hypersensitivity: studies in cell-mediated crescentic glomerulonephritis. J. Immunol. 2000; 165:4649–4657. [PubMed: 11035108]

39. Kitching AR, Turner AL, Wilson GR, Semple T, Odobasic D, Timoshanko JR, O'Sullivan KM, Tipping PG, Takeda K, Akira S, Holdsworth SR. IL-12p40 and IL-18 in crescentic glomerulonephritis: IL-12p40 is the key Th1-defining cytokine chain, whereas IL-18 promotes local inflammation and leukocyte recruitment. J. Am. Soc. Nephrol. 2005; 16:2023–2033. [PubMed: 15888563]

40. Bonniaud P, Margetts PJ, Ask K, Flanders K, Gauldie J, Kolb M. TGF-β and Smad3 signaling link inflammation to chronic fibrogenesis. J. Immunol. 2005; 175:5390–5395. [PubMed: 16210645]

41. Bamias G, Martin C, Mishina M, Ross WG, Rivera-Nieves J, Marini M, Cominelli F. Proinflammatory effects of TH2 cytokines in a murine model of chronic small intestinal inflammation. Gastroenterology. 2005; 128:654–666. [PubMed: 15765401]

42. Huaux F, Arras M, Tomasi D, Barbarin V, Delos M, Coutelier JP, Vink A, Phan SH, Renauld JC, Lison D. A profibrotic function of IL-12p40 in experimental pulmonary fibrosis. J. Immunol. 2002; 169:2653–2661. [PubMed: 12193738]

43. Na C-L, Duan CX, Apsley KS, Weaver TE. Abnormal alveolar type 2 cell phenotype in AP-3 mutant mocha and pearl mice: an electron microscopy study. Microsc. Microanal. 2003; 9:1426–1427.

44. Yoshioka Y, Kumasaka T, Ishidoh K, Kominami E, Mitani K, Hosokawa Y, Fukuchi Y. Inflammatory response and cathepsins in silica-exposed Hermansky-Pudlak syndrome model pale ear mice. Pathol. Int. 2004; 54:322–331. [PubMed: 15086836]

45. Horwitz M, Benson KF, Duan Z, Li FQ, Person RE. Hereditary neutropenia: dogs explain human neutrophil elastase mutations. Trends Mol. Med. 2004; 10:163–170. [PubMed: 15059607]

46. Benson KF, Li FQ, Person RE, Albani D, Duan Z, Wechsler J, Meade-White K, Williams K, Acland GM, Niemeyer G, et al. Mutations associated with neutropenia in dogs and humans disrupt intracellular transport of neutrophil elastase. Nat. Genet. 2003; 35:90–96. [PubMed: 12897784]

47. Akagawa KS, Kamoshita K, Tokunaga T. Effects of granulocyte-macrophage colony-stimulating factor and colony-stimulating factor-1 on the proliferation and differentiation of murine alveolar macrophages. J. Immunol. 1988; 141:3383–3390. [PubMed: 3053898]

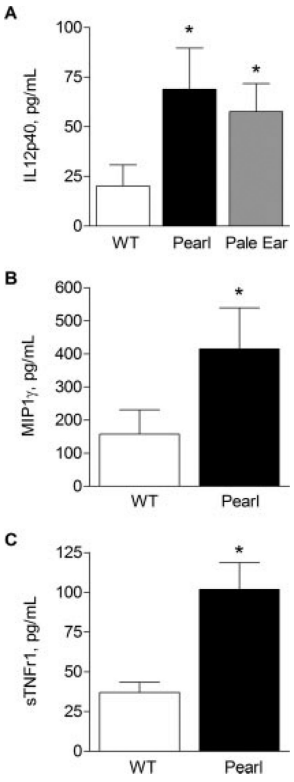

FIGURE 1.

Increased basal pulmonary cytokine and soluble TNFR levels in the BAL fluid of unchallenged HPS mice. BAL was performed in unchallenged pearl, pale ear, and WT mice (age 6–8 wk), and cytokine levels were assessed by ELISA (n = at least 8 animals for each point in *A*, and n = at least 12 animals for each point *B* and *C*).

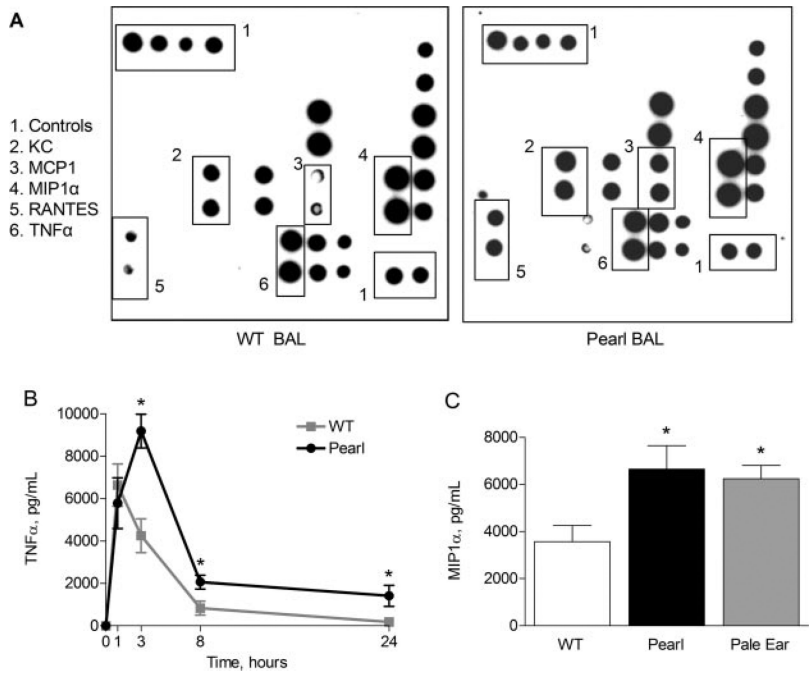

FIGURE 2.

Exaggerated and prolonged pulmonary cytokine responses in the BAL fluid of HPS mice after i.n. endotoxin administration. The lungs of pearl, pale ear, and WT mice (age 8–10 wk) were challenged with i.n. instillations of LPS (J5, 1 μg) or saline vehicle, and BAL was performed at various time points up to 24 h. Cytokine levels were assessed by protein array (*A*) or by ELISA (*B* and *C*) (n = at least 8 animals for each point for *B* and *C*). *A*, Cytokine protein array screen suggests increased TNF-α, MIP1α, MCP-1, RANTES, and KC levels in pearl vs WT BAL fluid 3 h after i.n. LPS. *B*, Levels of TNF-α in pearl (●) and WT (■) BAL fluid, up to 24 h after LPS (*, $p < 0.001$). *C*, Levels of MIP1α in WT, pearl, and pale ear BAL 3 h after LPS (*, $p < 0.001$ for pearl or pale ear vs WT).

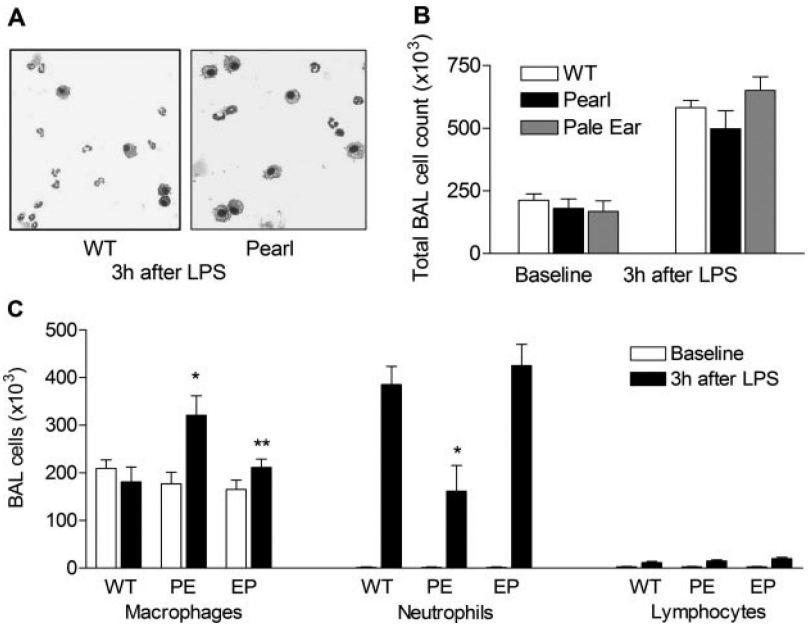

FIGURE 3.

BAL cell populations in HPS mice after i.n. endotoxin administration. *A*, Photomicrograph of WT and pearl cells recovered by BAL 3 h after LPS challenge. Note the excess of "foamy" macrophages but the paucity of polymorphonuclear cells (PMNs) in pearl BAL compared with WT BAL. *B*, Total BAL cell counts at baseline and 3 h after LPS challenge. *C*, BAL cell differentials at baseline and 3 h after i.n. LPS challenge. Note the relative lack of PMNs but excess macrophages in pearl BAL, compared with BAL from pale ear mice 3 h after LPS challenge (*, $p < 0.01$ for pearl vs pale ear or WT; **, $p < 0.05$ for pale ear baseline vs LPS).

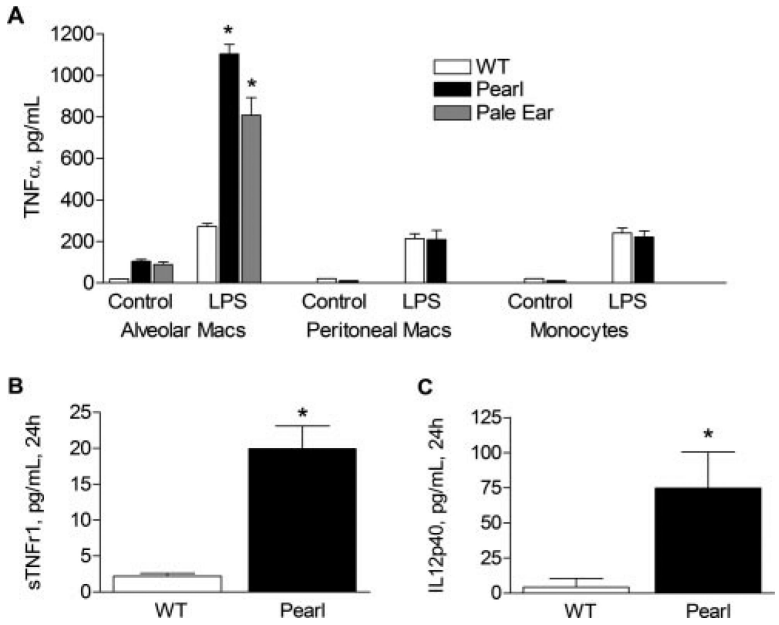

FIGURE 4.

Pearl AMs, but not peritoneal macrophages or peripheral monocytes, produce high levels of inflammatory cytokines and soluble TNFRs at baseline and in response to LPS challenge, ex vivo. Murine AMs, peritoneal macrophages, and peripheral monocytes were isolated and allowed to adhere to plastic for 30 min before the addition of LPS (1 μg/ml) or control vehicle. After 3.5 h (*A*) or 24 h (*B* and *C*), cell media was collected and levels of cytokines or soluble TNFRs in the media supernatant were measured by ELISA ($n = 10$ minimum each group; *, $p < 0.01$ for WT vs pearl or pale ear AM controls; **, $p < 0.001$ for pearl vs WT AMs + LPS). LPS-challenged pearl AMs also exhibited elevated levels of MIP1α and KC compared with WT AMs (data not shown). Studies were not performed in pale ear peritoneal macrophages or peripheral blood monocytes.

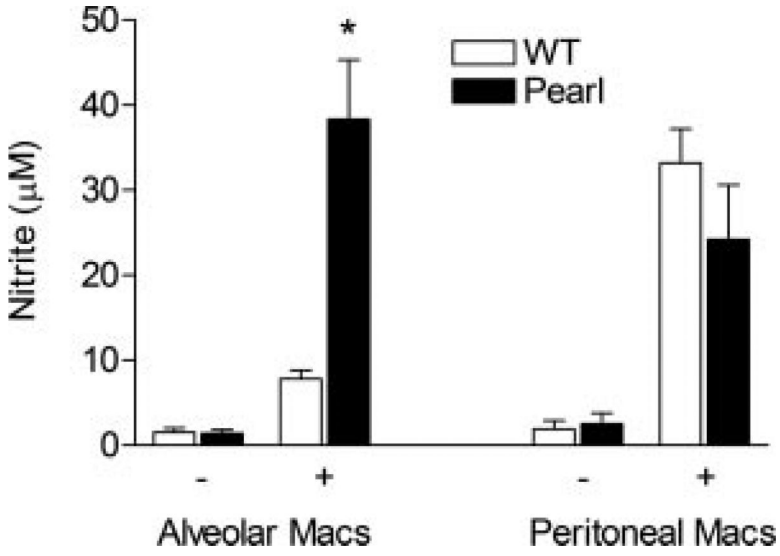

FIGURE 5.

Pearl AMs, but not peritoneal macrophages, produce high levels of NO in response to LPS challenge, ex vivo. Murine AMs and peritoneal macrophages were isolated and allowed to adhere to plastic before challenge with vehicle (–) or with IFN-γ/LPS (+) as indicated. After 24 h, cell media supernatant was collected and nitrite was quantitated by the Griess reaction (n = 3 separate experiments with replicates).

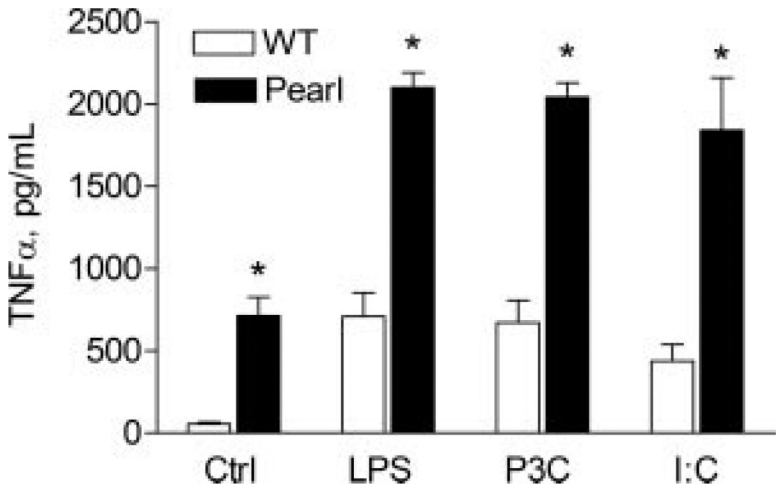

FIGURE 6.

Pearl AM hyperresponsiveness is not limited to TLR4 stimuli. Primary AMs were isolated from pearl and WT mice, and cells were stimulated in vitro with vehicle only (ctrl), repurified LPS (1 μg/ml), the TLR2 ligand Pam3Cys (1 μg/ml), or the TLR3 ligand poly(I:C) (50 μg/ml). After 4 h, cell media was collected and cytokine levels were measured by ELISA ($n = 4$ for controls; $n = 8$ for LPS and Pam3Cys; *, $p < 0.01$ for WT vs pearl).

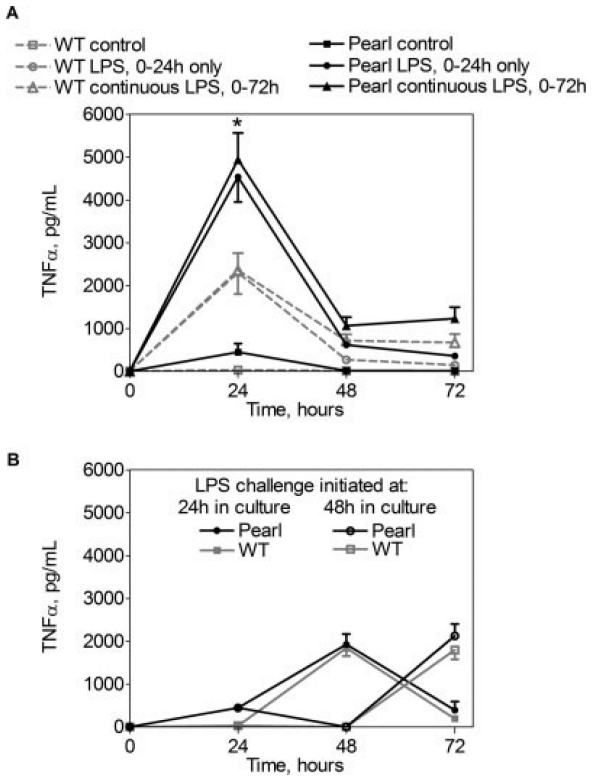

FIGURE 7.

Pearl AM hyperresponsiveness is lost after 24 h in culture. Primary AMs were isolated from pearl and WT mice, cultured for up to 72 h, and challenged with LPS (100 ng/ml) for various intervals (time 0–24, 24–48, 48–72 h, or continuously). Cell media was harvested and replaced with fresh media every 24 h, with or without LPS, and TNF-α levels were measured by ELISA. *A*, Pearl AMs produce TNF-α under control conditions (■), and exhibit LPS hyperresponsiveness compared with WT AMs when challenged for 0–24 h in culture (○ and ●). However, upon withdrawal of LPS at 24 h, or with continuous LPS exposure (△ and ▲), similar dampening of TNF-α production occurs in pearl and WT AMs. *B*, Pearl AMs have similar LPS responses as WT AMs when challenge with LPS is delayed until after 24 h (● and ■) or 48 h (○ and □) in vitro.

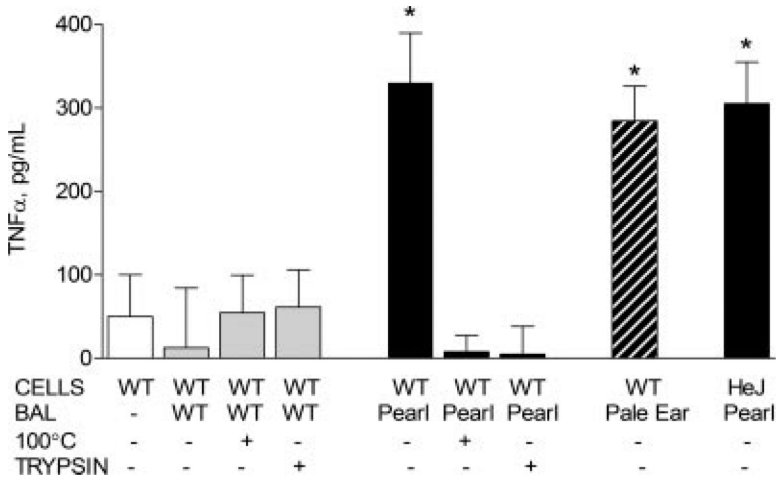

FIGURE 8.

Protein components of BAL from pearl mice activate WT macrophages. BAL was obtained from control pearl and WT mice, concentrated, and verified to be endotoxin-free by LAL assay. Primary AMs from WT mice were stimulated in vitro with concentrated WT, pearl, or pale ear BAL fluid (BAL total protein concentration of 0.5 μg/μl) for 3 h. In some experiments as indicated, BAL fluid was boiled (100°C) or treated with trypsin (1 μg, 37°C, 1 h) before addition to cells. AMs from C3H/HeJ mice, which contain a TLR4 mutation and thus do not respond to LPS, were also activated by exposure to pearl BAL (n = 12 each group for BAL; n = 4 each for boiling and trypsin; n = 4 for HeJ; *, $p < 0.001$).